Available online at www.sciencedirect.com
ScienceDirect
International Journal of Heat and Mass Transfer 50 (2007) 3740–3748
International Journal of HEAT and MASS TRANSFER
www.elsevier.com/locate/ijhmt

A heat transfer model for the analysis of transient heating of the slab in a direct-fired walking beam type reheating furnace

Man Young Kim *

School of Mechanical and Aerospace Systems Engineering, Research Center of Industrial Technology, Chonbuk National University, 664-14 Duckjin-Dong, Duckjin-Gu, Jeonju, Chonbuk 561-756, Republic of Korea

Received 24 March 2006; received in revised form 16 February 2007
Available online 20 April 2007

Abstract

A mathematical heat transfer model for the prediction of heat flux on the slab surface and temperature distribution in the slab has been developed by considering the thermal radiation in the furnace chamber and transient heat conduction governing equations in the slab, respectively. The furnace is modeled as radiating medium with spatially varying temperature and constant absorption coefficient. The steel slabs are moved on the next fixed beam by the walking beam after being heated up through the non-firing, charging, preheating, heating, and soaking zones in the furnace. Radiative heat flux calculated from the radiative heat exchange within the furnace modeled using the FVM by considering the effect of furnace wall, slab, and combustion gases is introduced as the boundary condition of the transient conduction equation of the slab. Heat transfer characteristics and temperature behavior of the slab is investigated by changing such parameters as absorption coefficient and emissivity of the slab. Comparison with the experimental work show that the present heat transfer model works well for the prediction of thermal behavior of the slab in the reheating furnace.

Keywords: Reheating furnace; Steel slab heating; Radiative heat transfer; Transient heat conduction; Finite volume method

1. Introduction

The analysis of transient heating characteristics of the steel slabs in a reheating furnace has attracted considerable attention during the past few decades since the furnace process should have lower energy consumption and pollutant emissions. In addition, requirement of the uniform temperature distributions inside the slab at the furnace exit greatly increases the importance of accurate and fast prediction of furnace process for the subsequent rolling process because this determines the quality of the steel product. Intrinsically, the combustion process and resulting hot gas flow within the furnace chamber influence the heat transfer process through conduction, convection, and thermal radiation simultaneously. However, complex three dimensional structure of the furnace including stationary and walking skids makes the problem difficult to analyze accurately and economically. Therefore, models and methods for predicting the furnace combusting behavior and heat transfer processes are in high demand. Especially, accurate prediction of thermal radiation behavior is quite important because the heat transfer by thermal radiation is over 90% of the total heat flux impinging on the slab surface [1].

Now that no single radiation model can solve all situations encountered in engineering applications, one should select an appropriate approach for his own specific concern. In order to predict the radiative heat flux on the slab surface, thereby, calculate the temperature distribution inside a slab accurately, its solution method must account for the sequential slab movement, nongray behavior of the furnace radiating gases, and complex geometry including curved furnace wall and blockage effect of slab and skid pipes, as well as moderate computational cost. Numerous

* Tel.: +82 63 270 2473; fax: +82 63 270 2472.
E-mail address: manykim@chonbuk.ac.kr

0017-9310/$ - see front matter © 2007 Elsevier Ltd. All rights reserved.
doi:10.1016/j.ijheatmasstransfer.2007.02.023

Nomenclature

D_i^m	directional weights in direction m at surface i, Eq. (11)
I	actual radiation intensity, W/(m^2 sr)
I_b	blackbody radiation intensity, $= \sigma T^4/\pi$, W/(m^2 sr)
k	conductivity of slab, W/(m K)
M	total number of radiation direction
$\vec{n}_i$	outward unit normal vector at surface i
q^R_{slab}	radiative heat flux at the slab surface, W/m^2, Eqs. (2) and (18)
$\vec{r}$	position vector
$\vec{s}$	unit direction vector
T	temperature, K
t	time, s
x, y	axes of Cartesian coordinate

Greek symbols

β_0	extinction coefficient, $= \kappa_a + \sigma_s$, m^{-1}
$\Delta A_i, \Delta V$	surface area and volume of the control volume, respectively
$\Delta\Omega^m$	discrete control angle, sr
ε_w	wall emissivity
θ	polar angle measured from the z-axis, rad
κ_a	absorption coefficient, m^{-1}
σ	Stefan–Boltzmann constant, $= 5.67 \times 10^{-8}$ W/(m^2 K^4)
σ_s	scattering coefficient, m^{-1}
Φ	scattering phase function
ϕ	azimuthal angle measured from the x-axis, rad
ω_0	scattering albedo, $= \sigma_s/\beta_0$

Subscripts

E, W, N, S	east, west, north, and south neighbors of P, see Fig. 4
e, w, n, s	east, west, north, and south control volume faces, see Fig. 4
P	nodal point in which intensities are located, see Fig. 4
w	wall

Superscript

m, m'	radiation direction

practical engineering models and methods for the prediction of thermal heating characteristics of the slab in a reheating furnace have been developed and successfully applied to various different furnace geometries [1–7], and these can be classified as below several categories.

The first one is to solve the full Navier–Stokes and energy conservation equations governing the hot gas flow and combustion process in the furnace, where thermal radiation acts as an energy source term via divergence of radiative heat flux. Kim et al. [1] performed these three dimensional CFD analysis by considering the turbulent reactive flow and radiative heat transfer in the walking beam type slab reheating furnace by using the commercial FLUENT code, and predicted temperature distribution in the furnace and heat fluxes through the upper and lower surface of the slabs. Kim and Huh [2] conducted similar analysis and predicted the thermal behavior of the slab by considering the transient conduction equation in the slab. Although these full CFD analyses can be used for accurate prediction of the thermal and combusting fluid characteristics in the furnace with slab heating, there exist such difficulties as treatment of so many governing equations and complexity of the furnace structure as well as uncertainty of the models, therefore, it necessitates long computational time and resulting costs. The second method models the furnace process as several well-stirred gas zones with one dimensional gas energy balance as suggested by Chapman et al. [4]. They performed the parametric investigations to find the effects of slab and refractory wall emissivities and height of the combustion space on the thermal performance of the continuous reheating furnace. They did not, however, predict the temperature distribution inside the slab, and some modifications are needed to deal with the complex furnace geometry and walking beam type reheating furnace considered in this work. The final approach, which is simple but can reasonably simulate the thermal behavior of the slab, is to focus on the analysis of radiative heat transfer of furnace gas and transient heat conduction within the slab [5–7]. Li et al. [5] developed the mathematical model for predicting steady state heat transfer within the reheating furnace, where thermal radiation in a furnace gas is calculated by using the zone method, while the thermal response of the slab is obtained by solving the transient two dimensional conduction equation. To the author's knowledge, however, the computing cost of the zone method is expensive and extension to general body-fitted coordinates to deal with the complex furnace structure is somewhat difficult. Yang et al. [6] also developed the similar heat transfer model and predicted the temperatures in the slab with skid pipes by considering quasi-steady two dimensional heat transfer transverse to the marching direction of the slab in the reheating furnace. Although it is more simple and less computational time is required compared with the approach of Li et al. [5], more general and computationally efficient model is highly demanded for the fast and accurate temperature prediction of the slab, if considering the useful on-line model which monitors and controls the furnace situations like control of the burner and residence time of the slab within the furnace for real time operation.

Recently, Harish and Dutta [7] presented a computational model for the heat transfer in a direct-fired pusher type reheat furnace by using the FVM for gas radiative heat transfer and WSGGM for nongray behavior of the combustion gases within the furnace. In this work, a mathematical heat transfer model to predict the radiative heat flux impinging on the slab surface and temperature distribution inside the slab has been developed by considering the thermal radiation in the furnace chamber and transient conduction governing equations in the slab in the walking beam type reheating furnace, respectively. The furnace is modeled as radiating medium with spatially varying temperature and constant absorption coefficient. The slab is moved on the next fixed beam by the walking beam periodically passing through the non-firing, charging, preheating, heating, and soaking zones in the furnace. Radiative heat flux calculated from the radiative heat exchange within the furnace chamber modeled using the finite volume method for radiation by considering the effect of furnace wall, slab, and combustion gases is applied as the boundary condition of the transient heat conduction equation of the slab. In the following sections after describing the methodology adopted here for the prediction of furnace process within the reheating furnace, heat transfer characteristics and thermal behavior of the slab are investigated by changing such parameters as absorption coefficient and emissivity of the slab, while comparison with the experimental data is also presented. Finally, some concluding remarks are given.

2. Formulation

2.1. Furnace description

The role of the reheating furnace is to heat steel slabs nearly up to 1200 °C uniformly for the subsequent rolling process, and the energy for slab heating is supplied by roof and bottom tangential gas burners. Usually, this reheating furnace is composed of five zones, i.e., non-firing, charging, preheating, heating, and soaking zones as shown in Fig. 1, which is the simplified furnace model similar to the POSCO unit. Steel slabs charged into the non-firing zone are moved on the next fixed beam by a walking beam about every some minutes depending on the residence time of the slab within the furnace. Overall longitudinal furnace dimension is in the order of 39.2 m, while the furnace height is varied at each zone with inclined connecting roof and block-shaped bottom hill. Each Steel slab has 1.16 m in width and 0.23 m in height with 0.2 m interval between the slabs, so that, there exist total 28 slabs in the present furnace. The steel slabs are assumed to be isothermal of 21.2 °C when charged into the furnace. Slab residence time, i.e., from charging into the furnace to exit from the furnace, is typically 180 min to obtain the mean slab temperature of about 1200 °C at the furnace exit, therefore, slabs move to the next location every 4.6 min.

2.2. Governing equations

Fig. 2 shows the heat transfer path occurred within the furnace chamber, in this study, it is assumed that the heat transfer mode to the slab surface is only thermal radiation while only conduction occurs within the slab. Heat transfer within the steel slab can be calculated from the transient two dimensional heat conduction equation as following:

$$\rho C \frac{\partial T}{\partial t} = \frac{\partial}{\partial x}\left(k \frac{\partial T}{\partial x}\right) + \frac{\partial}{\partial y}\left(k \frac{\partial T}{\partial y}\right) \tag{1}$$

where ρ, C, and k are density, specific heat, and conductivity of the steel slab, respectively. The radiative heat flux on the slab surface, q^{R}_{slab} as shown in Fig. 3, is used for the boundary condition of the above Eq. (1), i.e.,

$$q^{R}_{slab} = \int_{\Omega=4\pi} I(\vec{r}_w, \vec{s})(\vec{s} \cdot \vec{n}_w)\, d\Omega \tag{2}$$

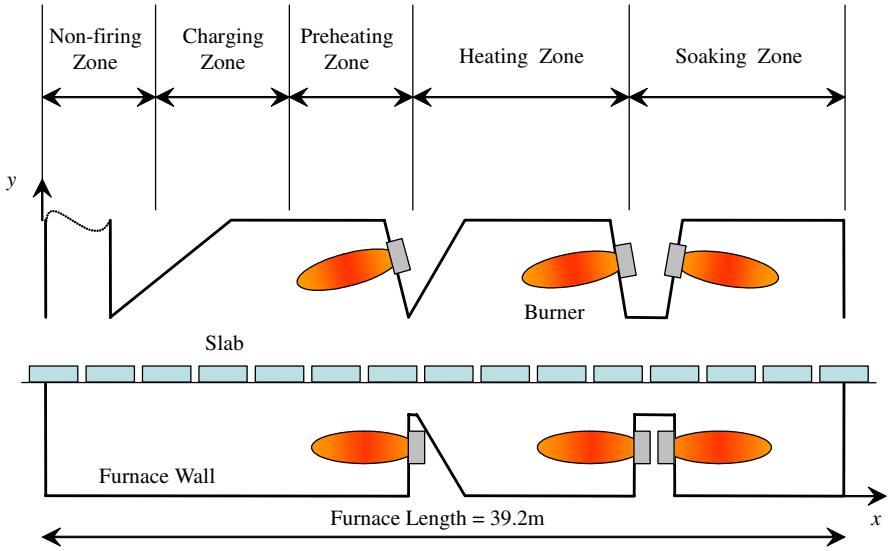

Fig. 1. Geometry of the model reheating furnace.

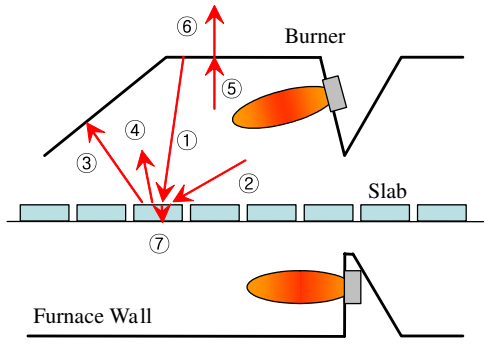

Fig. 2. Schematic of the heat transfer mechanism in the reheating furnace.

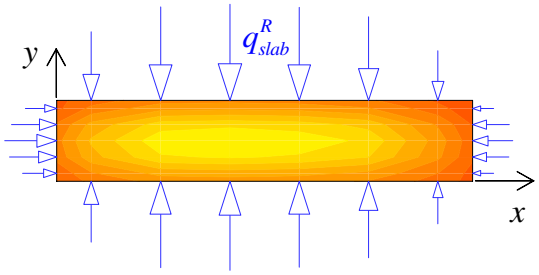

Fig. 3. Schematic of the slab geometry showing the radiative heat flux on the slab surface.

where $I(\vec{r}_w,\vec{s})$ is the radiation intensity at slab surface $\vec{r}_w$ and direction $\vec{s}$, $\vec{n}_w$ is the unit normal vector at the slab surface, and Ω is the solid angle. For a radiatively active medium the radiation intensity at any position $\vec{r}$, along a path $\vec{s}$ through an absorbing, emitting and scattering medium can be given by the following RTE:

$$\frac{1}{\beta_0}\frac{dI(\vec{r},\vec{s})}{ds} = -I(\vec{r},\vec{s}) + (1-\omega_0)I_b(\vec{r}) + \frac{\omega_0}{4\pi}\int_{\Omega'=4\pi} I(\vec{r},\vec{s})\Phi(\vec{s}'\to\vec{s})\,d\Omega' \quad (3)$$

where $\beta_0 = \kappa_a + \sigma_s$ is the extinction coefficient, $\omega_0 = \sigma_s/\beta_0$ is the scattering albedo, and $\Phi(\vec{s}'\to\vec{s})$ is the scattering phase function of radiative transfer from the incoming direction $\vec{s}'$ to the scattering direction $\vec{s}$. This equation, if the temperature of the medium $I_b(\vec{r})$ and boundary conditions for intensity are given, provides a distribution of the radiation intensity in medium. For a diffusely emitting and reflecting wall with temperature T_w, the outgoing intensity at wall which is the boundary condition of Eq. (3) can be expressed as the summation of emitted and reflected ones like:

$$I(\vec{r}_w,\vec{s}) = \varepsilon_w I_{bw}(\vec{r}_w) + \frac{1-\varepsilon_w}{\pi}\int_{\vec{s}'\cdot\vec{n}_w<0} I(\vec{r}_w,\vec{s})|\vec{s}'\cdot\vec{n}_w|\,d\Omega' \quad (4)$$

where ε_w is the wall emissivity, and $I_{bw} = \sigma T_w^4/\pi$ is the blackbody intensity of the wall.

2.3. Finite volume solution methods

The transient heat conduction equation is discretized by using the finite volume method following the procedure suggested by Patankar [8]. A central differencing scheme is used for the diffusion terms in the x and y directions, while the unsteady term is treated implicitly. The resulting discretized system is then solved iteratively by using the TDMA algorithm until the temperature field in the slab satisfies the following convergence criterion:

$$\max(|T_{i,j} - T^{old}_{i,j}|/T_{i,j}) \leqslant 10^{-6} \quad (5)$$

where $T^{old}_{i,j}$ is the previous iteration value of $T_{i,j}$ in the same time level.

In order to compute the radiative heat flux on the slab surface expressed in Eq. (2), which is the boundary condition of Eq. (1), the RTE, Eq. (3) must be analyzed. In this work, the finite volume method for radiation suggested by Chui and Raithby [9], and developed by Chai et al. [10] and Baek et al. [11] is adopted to discretize the RTE. To obtain the final discretization equation, after integrating the RTE over a control volume ΔV and control angle $\Delta\Omega^m$ as shown in Fig. 4a and b, respectively, with the assumption that the magnitude of intensity is constant within a control volume

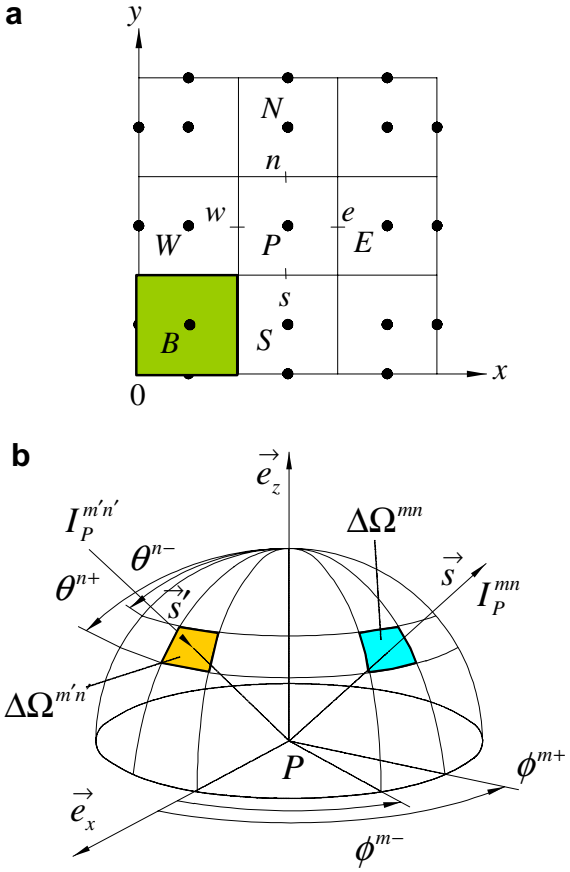

Fig. 4. Spatial control volume and control (solid) angles: (a) control volume, (b) control angle.

and a control angle given, but allowing its direction to vary, the following equation can be obtained:

$$a_P^m I_P^m = a_E^m I_E^m + a_W^m I_W^m + a_N^m I_N^m + a_S^m I_S^m + b_P^m \tag{6}$$

where

$$a_I^m = \max(-\Delta A_i D_i^m, 0) \tag{7}$$

$$a_P^m = \sum_{i=e,w,n,s} \max(\Delta A_i D_i^m, 0) + \beta_{0,P} \Delta V \Delta \Omega^m \tag{8}$$

$$b_P^m = (S_R^m)_P \Delta V \Delta \Omega^m \tag{9}$$

$$S_R^m = \kappa_a I_b + \frac{\sigma_s}{4\pi} \int_{\Omega'=4\pi} I^{m'} \Phi^{m' \to m} \Delta \Omega^{m'} \tag{10}$$

$$D_i^m = \int_{\Delta \Omega^m} (\vec{s} \cdot \vec{n}_i)\, \mathrm{d}\Omega^m \tag{11}$$

where ΔA_i and $\vec{n}_i$ are the surface area and outward unit normal vector at the surface i, respectively. Also, subscript I represents E, W, N and S, while i does e, w, n and s, respectively. Here is adopted a step scheme in which a downstream face intensity is set to equal to the upstream nodal value. The discretization procedure and related quantities are easily found in Baek et al. [11].

If the radiatively inactive regions such as slab in the furnace and block in the bottom furnace wall exist within the solution domain, like point B in Fig. 4a, the blocked-off procedure suggested by Chai et al. [10] can be adopted. In this treatment, although the calculation is done over the whole domain, only solutions in the active regions are meaningful. In order to explain the blocked-off treatment, an additional source term is introduced into Eq. (6) as follows [10,12]:

$$S^A = S_C^A + S_P^A I_P^m \tag{12}$$

For a cell in the inactive region it becomes $S_C^A = 0$ and $S_P^A = \mathrm{LN}$ (where LN is a large number, for example, 10^{20}), whereas in the active region, both S_C^A and S_P^A are set equal to zero. For an active cell in direct contact with an inactive cell, for example, point W in Fig. 4a, the following conditions are imposed:

$$S_C^A = -\frac{\Delta A_w D_w^m}{\Delta V \Delta \Omega^m} \left(\varepsilon_w I_{bw} + \frac{1-\varepsilon_w}{\pi} \sum_{m=1}^{M} I_w^m |D_w^m| \Delta \Omega^m \right) \tag{13}$$

$$S_P^A = 0 \tag{14}$$

Finally, the coefficients of Eqs. (8) and (9) are changed such that

$$a_P^m = \sum_{i=e,w,n,s} \max(\Delta A_i D_i^m, 0) + (\beta_{0,P} - S_P^A) \Delta V \Delta \Omega^m \tag{15}$$

$$b_P^m = (S_R^m + S_C^A)_P \Delta V \Delta \Omega^m \tag{16}$$

The iterative solution procedure is terminated when the following convergence is attained:

$$\max(|I_P^m - I_P^{m,\mathrm{old}}| / I_P^m) \leqslant 10^{-6} \tag{17}$$

where $I_P^{m,\mathrm{old}}$ is the previous iteration value of I_P^m.

Once the intensity field is obtained, the radiative heat flux on the slab surface in Eq. (2) can be estimated by using the directional weights D_w^m as follows:

$$q_{\mathrm{slab}}^R = \int_{\Omega=4\pi} I(\vec{r}_w, \vec{s})(\vec{s} \cdot \vec{n}_w)\, \mathrm{d}\Omega = \sum_{m=1}^{M} I_w^m D_w^m \tag{18}$$

To obtain the individual slab temperature in each time, the calculation starts from thermal radiation in the furnace chamber to give radiative heat flux on each slab surface. Then, heat conduction inside the slab is sequentially simulated from first to the final 28th slab. This calculation loop is repeated until the slab moves to the next fixed beam by a walking beam, and above mentioned calculation procedure is performed with the initial slab temperature of previously calculated one at that location. These calculation procedures are terminated when it becomes the residence time of the slab in the furnace.

3. Results and discussion

3.1. Thermal behavior of the furnace process

The reheating furnace heat transfer model with thermal radiation in the furnace chamber and transient heat conduction inside the slab presented above is applied to investigate several aspects of furnace behavior, especially, focusing on the slab temperature at each slab and radiative heat flux on the slab surface in the model five zone reheating furnace similar to the POSCO unit. The temperature of the furnace wall and gases within the chamber used for the simulation are listed in Table 1, and the thermophysical properties of the slab are given in Table 2, respectively. The fundamental radiative properties such as absorption coefficient of the radiating gases κ_a is 0.15 m^{-1}, and emissivities of the furnace wall are set to 0.75 and 0.5, respectively, while it is assumed that there is no scattering, i.e., $\sigma_s = 0$, therefore, $\omega_0 = 0$. The spatial mesh systems used in this study is $(N_x \times N_y) = (198 \times 29)$ and angular systems of $(N_\theta \times N_\phi) = (4 \times 12)$ for 2π sr. All calculations were conducted on a 1.7 MHz personal computer, and required computational time is about 1260 s.

Table 1
Temperature conditions used in this study [°C]

Zone	T_{w_upper}	T_{g_upper}	T_{g_lower}	T_{w_lower}
Non-firing	750	950	950	700
Charging	950	1150	1150	900
Preheating	1040	1240	1240	990
Heating	1050	1250	1230	980
Soaking	960	1160	1120	970

Table 2
Conductivity and specific heat of the slab

Temperature [°C]	Conductivity [W/m K]	Specific heat [J/kg K]
<30	26.89	299.0
400	25.44	401.6
600	22.70	512.0
800	20.89	542.8
1000>	23.69	478.9

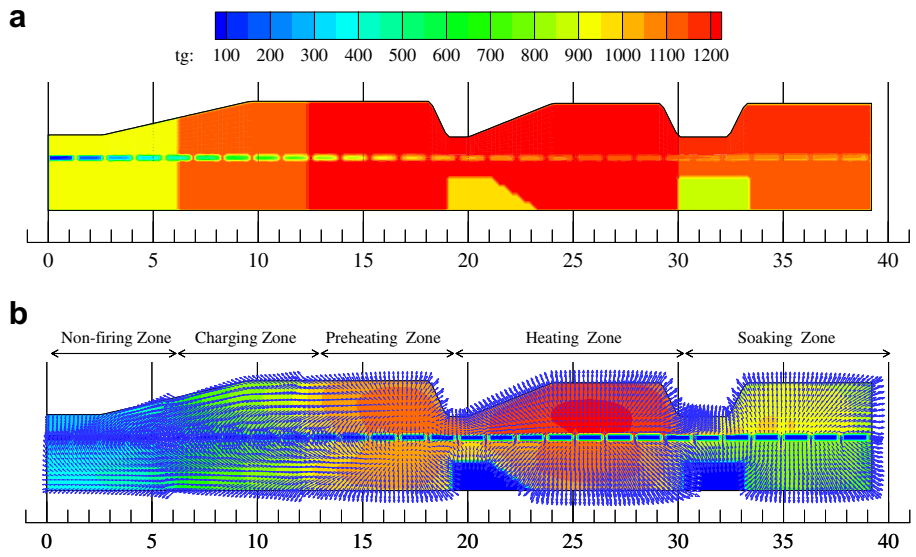

Fig. 5. Distribution of the (a) radiative heat flux vectors and incident radiation and (b) temperature (°C).

Fig. 5a illustrates the temperature distribution of the total 28 slabs with the five zone furnace temperature listed in Table 1. The first slab charged into the non-firing zone with 21.2 °C receives strong thermal radiation from neighboring hot furnace gases and wall because of relatively high temperature difference between the slab and others, and then heated up to maximum temperature of 346.1 °C at the right corner region of the slab. As is expected, the slabs are more heated up as passing through the subsequent charging, preheating, and heating zones nearly to 1150 °C. Temperature within the slab, however, is slightly lowered and somewhat equilibrated in the final soaking zone. Fig. 5b shows the radiation behavior in the furnace chamber, i.e., radiative heat flux (vectors) and incident radiation (contours). Note that in the first two zones radiative heat flux vectors are concentrated on the slab located at the near center of the furnace height, which means that a lot of heating is made in these early zones of the furnace. Steel slabs are more heated by passing through the adjacent preheating and heating zones, thereby, peak temperature appears in the heating zone. On the other hand, in the final soaking zone, because the furnace temperature is slightly down about 90 °C than the previous heating zone and the slab is in high temperature nearly to the furnace gas temperature, some radiative heat flux is emitted from the hot slab, which is the reverse phenomenon compared with the situation in the previous zones. Therefore, temperature of the slab is slightly lowered and the temperature gradient within the slab becomes smaller.

Above mentioned thermal behavior in the reheating furnace can be seen in detail in Fig. 6, where distribution of the radiative heat flux vectors on the slab surface and temperature contours inside the particular slab in each zone are illustrated. Here, direction of radiative heat flux vector is rearranged to show whether the net heat flux enters or leaves the surface of the slab. The first slab in Fig. 6a is in the entrance of the furnace, therefore, heat flux vector on the left side disappears. As going right end of the slab, however, more heat reaches the upper and lower surface of the slab because of hot neighboring gases in the furnace. Also it is noted that at both right corners heat fluxes come from both horizontal and vertical directions, thereby, as is expected, maximum temperature of 346.1 °C is formed in this corner region while minimum temperature is found in the left center region of the slab. On the other hand, although the third slab in Fig. 6b is in the same non-firing zone, more heat fluxes impinge on the slab surface from furnace chamber and wall because which is located in the inner part of the furnace than first slab. Therefore, the slab is more heated up to maximum 547.1 °C, and minimum temperature is also increases to 245.8 °C. As yet, however, temperature distribution shows the sharp gradient inside the slab. The 7th slab in Fig. 6c is in the charging zone, where the slab has temperature range between 583.9 °C and 925.5 °C. As the slab moves to the preheating zone, however, since the slabs are sufficiently heated up and thereby temperature difference between the slab and neighboring medium and furnace wall becomes small, magnitude of heat flux decreases as shown in Fig. 6d. At the same reason, the incoming heat flux more decreases in the 17th slab in heating zone as shown in Fig. 6e, therefore, temperature rise of the slab is weakened and temperature is more evenly distributed. Fig. 6f shows the 26th slab in the final soaking zone, where temperature of the medium and furnace wall decreases than the previous heating zone. Consequently, one can notice the occurrence of the back heat flow from the slab surface into its surroundings and temperature of the slab decreases more or less compared with the slab in the previous heating zone.

Further, displayed in Fig. 7 are the predicted temperature profiles of the slab along the longitudinal direction of the furnace, where *Ts_u*, *Ts_c*, and *Ts_d* denote the average temperature of the upper surface, centerline of the slab

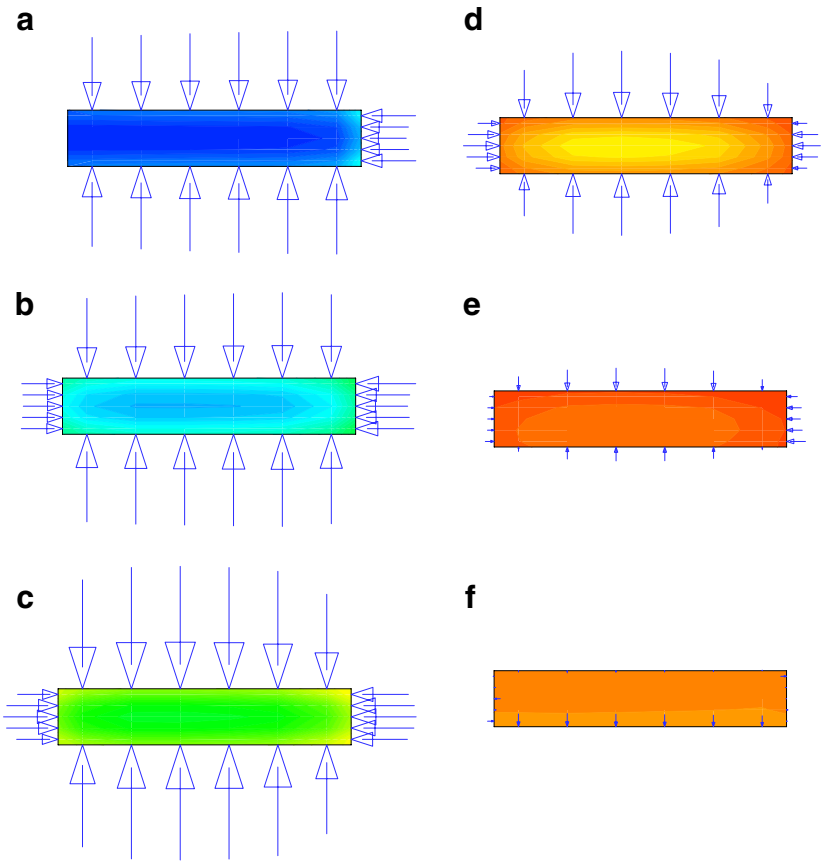

Fig. 6. Distribution of the radiative heat flux vector on the slab surface and temperature contours in the slab: (a) 1st slab, $T_{min} = 75.2\ ^{\circ}C$, $T_{max} = 346.1\ ^{\circ}C$, (b) 3rd slab, $T_{min} = 245.8\ ^{\circ}C$, $T_{max} = 547.1\ ^{\circ}C$, (c) 7th slab, $T_{min} = 583.9\ ^{\circ}C$, $T_{max} = 925.5\ ^{\circ}C$, (d) 12th slab, $T_{min} = 925.6\ ^{\circ}C$, $T_{max} = 1119.1\ ^{\circ}C$, (e) 17th slab, $T_{min} = 1075.9\ ^{\circ}C$, $T_{max} = 1145.4\ ^{\circ}C$, (f) 26th slab, $T_{min} = 1029.3\ ^{\circ}C$, $T_{max} = 1075.0\ ^{\circ}C$.

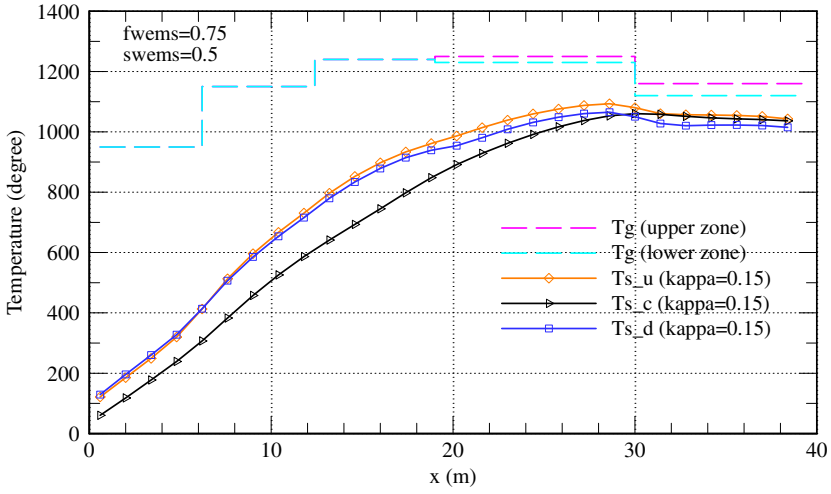

Fig. 7. Predicted temperature profiles of the slab along the axial direction of the furnace.

height, and lower surface of the slab, respectively. We can see that the centerline temperature of the slab charged into the furnace with 21.2 °C linearly increases through the first four zones from 60.4 °C to 1040.0 °C. In the final soaking zone, however, temperature slightly decreases and remains almost constant about 1010.0 °C. As for the upper and lower surface temperature it is found that although the upper temperature is slightly lower than the lower one in the first non-firing zone because of the lower cold furnace wall is more far from the slab, after charging zone the temperature reversal occurs and upper temperature is higher than lower one due to the existence of two cold blocks in the furnace bottom wall. On the contrary, in the final soaking zone, lower surface temperature is much lower than the

centerline temperature due to the above mentioned back heat flow.

3.2. Effect of absorption coefficient and slab emissivity

Radiative heat transfer from the flame and combustion gases and from the furnace wall to the slab is usually the dominant mode of heat transfer in high temperature reheating furnace. Here, to find the effect of radiative properties, some parametric studies are performed. Fig. 8 shows the effect of absorption coefficient of the medium on the longitudinal temperature profile of the centerline temperature of the slab. As shown, the slab centerline temperature increases as the absorption coefficient increases from 0.1 to 10.0 m^{-1}. This is because surrounding medium participates in thermal radiation more actively with the increase of the absorption coefficient. Next, the effect of slab emissivity on the temperature profile is introduced in Fig. 9, where slab emissivity is varied from 0.3 to 1.0, while absorption coefficient and furnace wall emissivity are kept at 0.15 m^{-1} and 0.75, respectively. As expected, temperature increases with the slab emissivity because the slab can receive more heat impinging on the surface as the surface becomes black. However, it is noted that although the effect of slab emissivity is more manifested within the furnace, the final temperature near exit is relatively in the narrow limits.

3.3. Comparison with the experimental data

Finally, the predicted temperature history in the slab using the present model is compared with the experimental data conducted by POSCO as shown in Fig. 10. In this figure, in situ measured average temperature in the upper and lower furnace zones, which is obtained by using each five k-type thermocouples located in the above and below the slab in the selected locations, is also presented with the centerline experimental data of the slab temperature. In order to predict the temperature of the slab, in situ measured temperature shown in Fig. 10 is used as medium temperature while furnace wall and slab emissivities are kept at 0.75

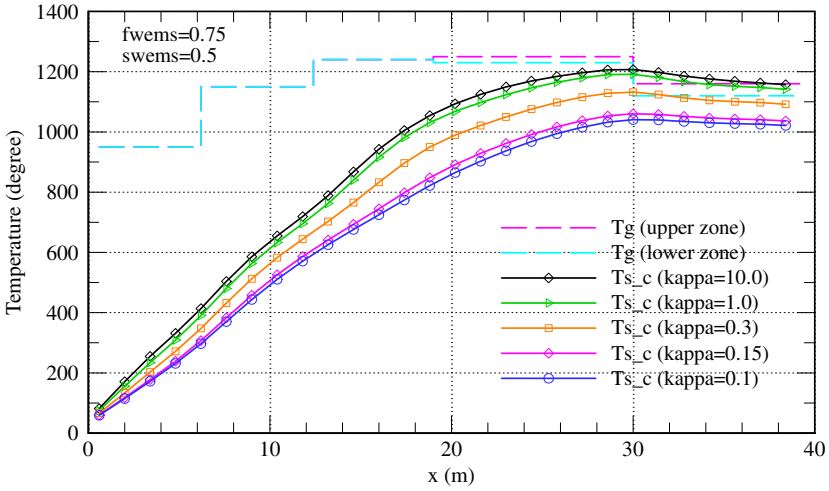

Fig. 8. Effect of absorption coefficient on the predicted longitudinal temperature profile of the slab.

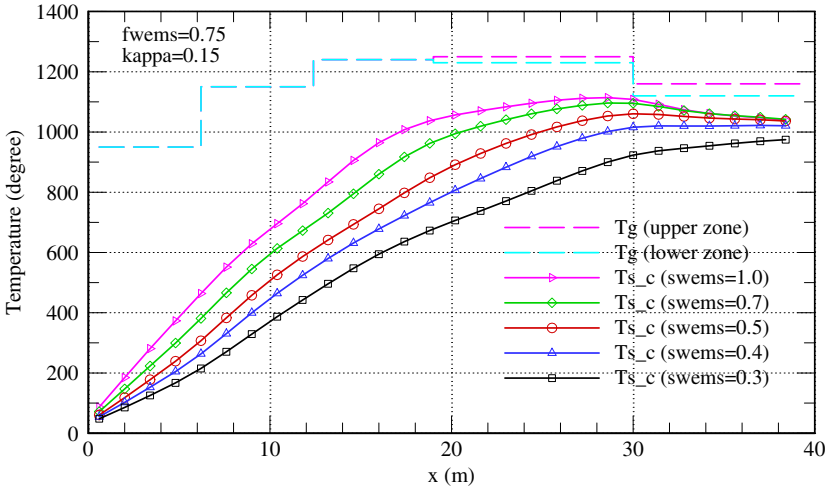

Fig. 9. Effect of slab emissivity on the predicted longitudinal temperature profile of the slab.

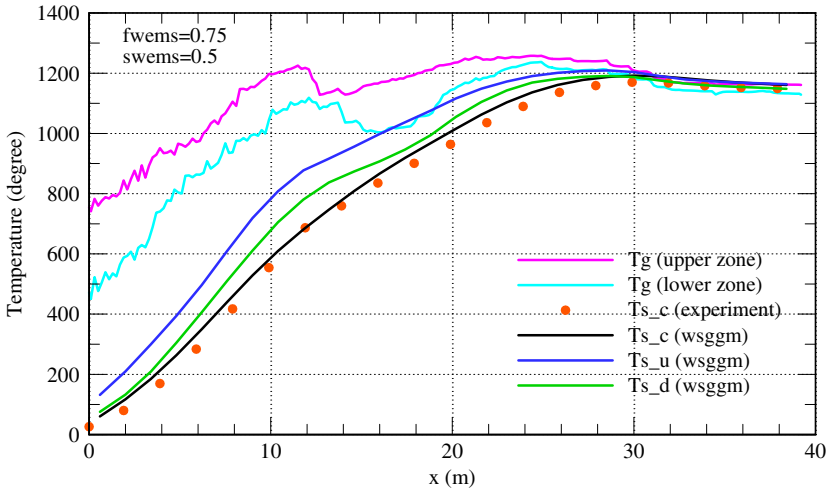

Fig. 10. Comparison of the predicted and measured longitudinal temperature profile of the slab.

and 0.5, respectively. Further, absorption coefficient of the medium is obtained by using he WSGG nongray model [13] based on the experimentally obtained CO_2 and H_2O mole fractions, which has similar value of the gray absorption coefficient of 0.15 m^{-1}. Note that although the uncertainty range of the measurements there exists a reasonable agreement between the predicted and measured temperature profiles. Especially, at the final soaking zone, namely near the exit of the furnace, the predicted temperature becomes to be in good agreement with the experimental data. This means that the present heat transfer model can be successfully applied to the walking beam type reheating furnace for the prediction of slab temperature.

4. Conclusions

A heat transfer model and applications have been presented for the prediction of thermal behavior in a five zone reheating model furnace resembling the POSCO unit. Based on the given longitudinal furnace gas and wall temperatures, the model can predict the radiative heat flux on the slab surface and the temperature distribution in the slab during the heating process by coupling the RTE and transient heat conduction equation.

Although the numerical results are for the specific example under consideration, the same methodology may be used to model any similar reheating furnace in the design phase or currently in operation. Further development of the present model will aim to include appropriate submodels for the analysis of skid mark formation, gas and wall temperature distribution, and, finally, full three dimensional heat transfer model.

Acknowledgements

The author gratefully acknowledges the financial support by the POSCO and Chonbuk National University, Korea. Also, the author would like to thank Mr. D.E. Lee, POSCO technical R&D center for his constructive comments and kind help.

References

[1] J.G. Kim, K.Y. Huh, I.T. Kim, Three-dimensional analysis of the walking-beam-type slab reheating furnace in hot strip mills, Numer. Heat Transfer, Part A 38 (2000) 589–609.
[2] J.G. Kim, K.Y. Huh, Prediction of transient slab temperature distribution in the re-heating furnace of a walking-beam type for rolling of steel slabs, ISIJ Int. 40 (2000) 1115–1123.
[3] A.M. Maki, P.J. Osterman, M.J. Luomala, Numerical study of the pusher-type slab reheating furnace, Scand. J. Metall. 31 (2002) 81–87.
[4] K.S. Chapman, S. Ramadhyani, R. Viskanta, Modeling and parametric studies of heat transfer in a direct-fired continuous reheating furnace, Metall. Trans. 22B (1991) 513–521.
[5] Z. Li, P.V. Barr, J.K. Brimacombe, Computer simulation of the slab reheating furnace, Can. Metall. Quarterly 27 (1988) 187–196.
[6] B.Y. Yang, C.Y. Wu, C.J. Ho, T.-Y. Ho, A heat transfer model for skidmark formation on slab in a reheating furnace, J. Mater. Process. Manufactur. Sci. 3 (1995) 277–295.
[7] J. Harish, P. Dutta, Heat transfer analysis of pusher type reheat furnace, Ironmaking Steelmaking 32 (2005) 151–158.
[8] S.V. Patankar, Numerical Heat Transfer and Fluid Flow, McGraw Hill, New York, 1980.
[9] E.H. Chui, R.D. Raithby, Computation of radiant heat transfer on a nonorthogonal mesh using the finite-volume method, Numer. Heat Transfer, Part B 23 (1993) 269–288.
[10] J.C. Chai, H.S. Lee, S.V. Patankar, Treatment of irregular geometries using a Cartesian coordinates finite-volume radiation heat transfer procedure, Numer. Heat Transfer, Part B 26 (1994) 225–235.
[11] S.W. Baek, M.Y. Kim, J.S. Kim, Nonorthogonal finite-volume solutions of radiative heat transfer in a three-dimensional enclosure, Numer. Heat Transfer, Part B 34 (1998) 419–437.
[12] D.Y. Byun, S.W. Baek, M.Y. Kim, Investigation of radiative heat transfer in complex geometries using blocked-off, multiblock, and embedded boundary treatments, Numer. Heat Transfer, Part A 43 (2003) 807–825.
[13] T.F. Smith, Z.F. Shen, J.N. Friedman, Evaluation of coefficients for the weighted sum of gray gases model, J. Heat Transfer 104 (1982) 602–608.